Coexistence of self-similar and anomalous scalings in turbulent small-scale solar magnetic fields.

Andrei Y. Gorobets

Leibniz-Institut für Sonnenphysik (KIS), Schöneckstr. 6, Freiburg 79104, Germany

Svetlana V. Berdyugina

Leibniz-Institut für Sonnenphysik (KIS), Schöneckstr. 6, Freiburg 79104, Germany

Istituto ricerche solari Aldo e Cele Daccò (IRSOL), Faculty of Informatics, Università della Svizzera italiana, 6605 Locarno, Switzerland

July 11, 2023

Abstract

We report an evidence that self-similarity and anomalous scalings co-exist in a turbulent medium, particularly in fluctuations of the magnetic field flux density in magnetized plasma of the solar photosphere. The structure function scaling exponents in the inertial range have been analyzed for fluctuations grouped according to the sign of the path-dependent stochastic entropy production. It is found that the scaling exponents for fluctuations with the positive entropy production follow the phenological linear dependence for the magnetohydrodynamic turbulence. For fluctuations with the negative entropy production, the scaling is anomalous.

In the lower solar atmosphere (photosphere), the evolution of magnetic fields is influenced by turbulent magnetoconvective motions of plasma, especially in regions with weak fields (≤ 0.1 Mx m^{-2}) of the so-called "quiet Sun", i.e. away from pores, sunspots, and their groups (active regions), where stronger magnetic fields suppress convective motions. The quiet Sun line-of-sight magnetic flux density (MFD) B_z is observed as a rapidly evolving, spatially intermittent (fractal) quantity in magnetic field maps (magnetograms) [7, 6, 36, 17, 9]. Photospheric magnetograms (Fig. 1) are recorded by space missions with a high cadence during several 11-year solar cycles. The range of physical parameters in the solar atmosphere provides a unique laboratory for unprecedented continuous high spatial resolution studies of dynamic magnetic phenomena [31]. In this Letter, we report a first empirical evidence for a dual character of the scaling law in temporal fluctuations of $B_z(t)$ when their statistical realizations are analysed separately according to the sign of the stochastic entropy production.

We employ an uninterrupted observation of the quiet Sun at the solar disk center obtained by the Helioseismic and Magnetic Imager (HMI) on board the Solar Dynamics Observatory (SDO) space mission [29, 30]. The analyzed time-series consists of $51,782$ magnetograms in the Fe I 617.3 nm line from 2019 December 11, 00:00:22 UT to 2020 January 06, 23:58:07 UT, with the instrument-fixed cadence $\Delta t = 45\,\mathrm{s}$. This is exactly 27 days, which is somewhat longer than one synodic rotation period of 26.24 days.

The magnetogram series is considered pixel-wise as discrete, time-ordered snapshots of magnetic flux evolution in the Eulerian frame of reference. In this context, every pixel as a probe in the field of view (FoV) provides a finite-length random realization of MFD fluctuations (also called trajectory or path)

$$\begin{aligned} B_z(t) &:= \big\{B_z(t_1), B_z(t_1+\Delta t), \ldots, B_z(t_1+n\Delta t)\big\} \\ &= \big\{b_1, b_2, \ldots, b_n\big\} = \{b_t\},\ \ t \in [1, n], \end{aligned} \tag{1}$$

where t is the local time index starting at the local origin t_1, n is the length of the trajectory. The trajectory is a set of identically distributed, signed, non-Gaussian, random variables; sign of b_t designates polarity of $B_z(t)$ at a given time instance, and n is the exponentially distributed random number. At a given pixel, the total number of trajectories $\{b_t\}$ is arbitrary. It depends on: the overall observation time, a particular solar magnetic field topology within FoV, and the noise cutoff. Statistical properties of trajectories are assumed to be homogeneous in space for the quiet Sun, at least with the HMI spatio-temporal resolution [1]. Hence, trajectories of different pixels contribute to the overall statistics equally.

The nature of B_z fluctuations enables analysis of fluctuations including a measure of their irreversibility. Namely, Δt-transitions in $\{b_t\}$ obey Markov property [12], and so allow computing trajectory-dependent (total) stochastic entropy production

$$\Delta s_{\mathrm{T}}(\{b_t\}) = \ln\left[\frac{p_n\left(b_1, b_2, \cdots, b_n\right)}{p_n\left(b_n, \cdots, b_2, b_1\right)}\right] \tag{2}$$

$$= \ln\left[\frac{p(b_1)}{p(b_n)}\prod_{k=1}^{n-1}\frac{p(b_{k+1}|b_k)}{p(b_k|b_{k+1})}\right], \tag{3}$$

where p, p_n and $p(b_j|b_i)$ are respectively the marginal, n-joint and Δt-step conditional probability density functions (PDF). The random quantity Δs_{T} is the

[1] The empirical test of Markov property at a higher resolution in [12] revealed that granular and intergranular B_z had, to some extent, different statistical properties, which were neglected at that stage of the studies. More details of the relevant discrepancies were reported in [9].

measure of irreversibility of the trajectory, and its PDF has an exact symmetry relation, known as the detailed fluctuation theorem [2]:

$$\frac{p(\Delta s_{\mathrm{T}} > 0)}{p(\Delta s_{\mathrm{T}} < 0)} = e^{|\Delta s_{\mathrm{T}}|}. \tag{4}$$

That is, the total entropy consumption, $\Delta s_{\mathrm{T}}^{-} \equiv \Delta s_{\mathrm{T}} < 0$, is exactly exponentially less probable than the total entropy generation, $\Delta s_{\mathrm{T}}^{+} \equiv \Delta s_{\mathrm{T}} > 0$, of the same magnitude $|\Delta s_{\mathrm{T}}|$. Hereafter, the corresponding signs are placed as superscripts in notations of estimated quantities. The detailed pixel calculus and Markov property test for $\{b_t\}$ at a higher spatial resolution are described in [12]. For HMI $\{b_t\}$, properties of the regular Markov chains were considered in [11], and the validity of the fluctuation theorems (including Eq. (4)) was shown in [10].

Henceforth, in our investigation of scale invariance of $B_z(t)$ fluctuations due to turbulent origin, we take into account the sign of Δs_{T}, which defines two disjoint sets $\{b_t\}^{\pm}$. The conventional method of studying manifestations of scale invariance involves an analysis of signal's self-similarity in terms of the q-order structure functions (SF)

$$S_q(\ell) \equiv \langle |\delta_\ell B_z(t)|^q \rangle = \langle |B_z(t+\ell) - B_z(t)|^q \rangle, \tag{5}$$

where $\delta_\ell(\cdot)$ is an increment of a turbulent quantity at two points of the flow at a distance ℓ. The Taylor's "frozen turbulence" hypothesis connects temporal and spatial scales in measurements, so scales in Eq.(5) are used in units of spatial distance. The solar data we investigate do not resolve all vector components of the observable/inferred quantities like photospheric velocity and magnetic fields, and consequently details of real flows are quite uncertain. However, we assume that Taylor's hypothesis is applicable for MFD of the quiet Sun [14]. For the set of 1D trajectories of a finite length, SF are computed as the ensemble average, and ℓ is expressed in units of the sampling interval Δt.

The phenomelogical theory of turbulence establishes fundamental scaling relations for observable quantities, and hence defines power-law dependencies between SF. The Kolmogorov phenomenology [21] of the fully developed hydrodynamic (HD) turbulence at a high Reynolds number $R = v\ell_0/\nu$ predicts the scaling law in the inertial range $\lambda \ll \ell \ll \ell_0$:

$$\delta_\ell v \sim \varepsilon^{\frac{1}{3}} \ell^{\frac{1}{3}}, \tag{6}$$

where v is the velocity, ε is the average energy dissipation rate, ν is the viscosity, and ℓ_0 and λ are the integral and dissipation scales, respectively.

Turbulence of a magnetized plasma is described in the framework of magnetohydrodynamics (MHD). The corresponding Iroshnikov-Kraichnan phenomenology [16, 22] includes the Alfvén wave effect of coupling between velocity and magnetic field fluctuations on small-scales by the integral-scale magnetic field

[2]For introduction and review see, for example: [4, 15, 24, 18, 32, 19, 33]

B_0 [3, 28]. At a high magnetic Reynolds number $Rm = v_A l_0/\eta$, the self-similar scaling exponents are

$$\delta_\ell v \sim \delta_\ell B \sim [\varepsilon v_A]^{\frac{1}{4}} \ell^{\frac{1}{4}}, \tag{7}$$

where η is the magnetic diffusivity, $v_A \equiv B_0(4\pi\rho)^{-\frac{1}{2}}$ is the Alfvén velocity in B_0, ρ is the mass density, and $\ell_0 = v_A^3 \varepsilon^{-1}$.

In terms of SF, the self-similar (linear) scalings in Eqs. (6-7) read

$$S_q(\ell) \sim \ell^{\xi(q)}, \;\; \xi(q) = \frac{q}{m}, \tag{8}$$

with $m = 3$ for HD and $m = 4$ for MHD turbulence.

To cope with experimental limitations and irregularities of flows which hinder the analysis of scaling in $S_q(\ell)$, the concept of the Extended Self-Similarity (ESS) was proposed in Refs. [2, 1]. In essence, ESS is a set of the functional dependencies of SF of any order on SF of the order for which $\xi(q) = 1$. Hence, for the case of MHD turbulence we focus on ESS with the relative exponents ξ_4

$$S_q(\ell) \sim [S_4(\ell)]^{\xi_4(q)}, \;\; \xi_4(q) = \frac{\xi(q)}{\xi(4)}. \tag{9}$$

The linear scalings in Eq. (8) are violated by spatial inhomogeneities of the dissipation on small scales, as said by intermittency. Thus, the scaling exponents (anomalously) deviate from the exact linear relations, as has become evident from extensive experimental and numerical studies [8]. Models for intermittency differ by assumptions about statistical properties of the energy dissipation rate ε, such as log-normal [20], multifractal [25], and log-Poisson [35, 34]. The latter was revealed for the solar wind MHD turbulence [13, 26] and applied for photospheric flows [5]. The "standard model" of Ref.[26] as the non-parametric version of the log-Poisson model for MHD turbulence

$$\xi_4(q) = q/8 + 1 - (1/2)^{q/4} \tag{10}$$

is used as a reference for anomalous scaling in the results presented below.

In Fig. 2, the SF scalings are shown according to Eq. (9) being computed separately for two sets $\{b_t\}^{\pm}$. The discrepancy in slopes with respect to sign of Δs_{T} is clearly seen, especially for higher orders. Following ideas from Ref. [37], the inertial range is defined as the range in which Kolmogorov's $\frac{4}{5}$ law $S_3(\ell) = -\frac{4}{5}\varepsilon\ell$ holds. For our data, we found the inertial range to be from $15\Delta t$ to $19\Delta t$.

The range boundaries were modified by $\pm\Delta t$, to compensate for a rather coarse sampling rate Δt, because linear fits showed substantial variations with range boundaries. This modification also helps to improve statistics of fits. Therefore, an SF scaling (Eq. 9) in the inertial range is estimated by the set of independent linear fits within the extended inertial range $[15\Delta t \pm \Delta t, 19\Delta t \pm \Delta t]$. The ultimate value of the scaling exponent ξ_4 is then computed as the weighted mean of 9 exponents for every combination of the inertial range boundary variations given by $(0, \pm 1)\Delta t$.

This procedure was applied to three groups of fluctuations: $\{b_t\}^{\pm}$ and their joint data set. The result is shown in Fig. 3. Statistical robustness of the result is highlighted by the 99, 99% confidence level computed by the χ^2 minimization. Errors of the means are smaller than symbols and not shown.

Summarizing, an anomalous scaling is the intrinsic property of the MFD fluctuations in the quiet Sun (diamonds in Fig. 3). The main results is the statistically significant difference between $\xi^+(q)$ and $\xi^-(q)$. The former exhibits scaling exponents rather distinctly following the linear dependence $\frac{q}{4}$, in accordance with the Iroshnikov-Kraichnan phenomenology. Contrastly, fluctuations along Δs_{T}^--trajectories have anomalous scaling exponents, and the curve of $\xi^-(q)$ resembles the MHD log-Poisson model (Eq. 10). However, we note that models describing curves of $\xi(q)^-$ and $\xi(q)$ are out of the scope of the present Letter.

Following the arguments of She and Leveque [35], one can interpret our finding that entropy consuming fluctuations could be related to entropy (energy) sinks which support building up of coherent structures at larger scales due to correlations induced by intermittency. Correspondingly, entropy generating fluctuations are related to dissipation processes according to the phenomenological cascade model.

To conclude, splitting measurements according to the sign of the entropy production allows detecting an unexpected coexistence of self-similar and anomalous scalings in the inertial range of turbulent small-scale photospheric magnetic fields on the Sun. Future numerical and experimental/observational applications of the method proposed in this Letter may advance understanding of the self-similarity in turbulent phenomena.

We thank Petri Käapylä for stimulating discussions. Solar Dynamics Observatory (SDO) is a mission for NASA's Living With a Star (LWS) program. The Helioseismic and Magnetic Imager (HMI) data were provided by the Joint Science Operation Center (JSOC).

References

[1] R. Benzi, S. Ciliberto, C. Baudet, G. Ruiz Chavarria, and R. Tripiccione. Extended Self-Similarity in the Dissipation Range of Fully Developed Turbulence. *Europhysics Letters*, 24(4):275, November 1993.

[2] R. Benzi, S. Ciliberto, R. Tripiccione, C. Baudet, F. Massaioli, and S. Succi. Extended self-similarity in turbulent flows. *Physical Review E*, 48(1):R29–R32, July 1993.

[3] D. Biskamp. Cascade models for magnetohydrodynamic turbulence. *Physical Review E*, 50(4):2702–2711, October 1994.

[4] Carlos Bustamante, Jan Liphardt, and Felix Ritort. The nonequilibrium thermodynamics of small systems. *Physics Today*, 58(7):43–48, 2005.

[5] G. Consolini, F. Berrilli, E. Pietropaolo, R. Bruno, V. Carbone, B. Bavassano, and G. Ceppatelli. Characterization of the Solar Photospheric Velocity Field: A New Approach. In *Magnetic Fields and Solar Processes*, volume 448 of *ESA Special Publication*, page 209, December 1999.

[6] G. Consolini, V. Carbone, F. Berrilli, R. Bruno, B. Bavassano, C. Briand, B. Caccin, G. Ceppatelli, A. Egidi, I. Ermolli, A. Florio, G. Mainella, and E. Pietropaolo. Scaling behavior of the vertical velocity field in the solar photosphere. *Astronomy and Astrophysics*, 344:L33–L36, April 1999.

[7] M. Faurobert-Scholl, N. Feautrier, F. Machefert, K. Petrovay, and A. Spielfiedel. Turbulent magnetic fields in the solar photosphere: Diagnostics and interpretation. *Astronomy and Astrophysics*, 298:289, June 1995.

[8] Uriel Frisch. *Turbulence*. 1995.

[9] F. Giannattasio, G. Consolini, F. Berrilli, and P. De Michelis. Scaling properties of magnetic field fluctuations in the quiet Sun. *Astronomy & Astrophysics*, 659:a180, 2022.

[10] A. Y. Gorobets and S. V. Berdyugina. Stochastic entropy production in the quiet Sun magnetic fields. *Monthly Notices of the Royal Astronomical Society: Letters*, 483(1):L69–L74, February 2019.

[11] A. Y. Gorobets, S. V. Berdyugina, T. L. Riethmüller, J. Blanco Rodríguez, S. K. Solanki, P. Barthol, A. Gandorfer, L. Gizon, J. Hirzberger, M. van Noort, J. C. Del Toro Iniesta, D. Orozco Suárez, W. Schmidt, V. Martínez Pillet, and M. Knölker. The Maximum Entropy Limit of Small-scale Magnetic Field Fluctuations in the Quiet Sun. *The Astrophysical Journal Supplement Series*, 233(1):5, 2017.

[12] A. Y. Gorobets, J. M. Borrero, and S. Berdyugina. Markov Properties of The Magnetic Field in The Quiet Solar Photosphere. *The Astrophysical Journal*, 825(2):L18, July 2016.

[13] R. Grauer, J. Krug, and C. Marliani. Scaling of high-order structure functions in magnetohydrodynamic turbulence. *Physics Letters A*, 195(5):335–338, December 1994.

[14] J. A. Guerra, A. Pulkkinen, V. M. Uritsky, and S. Yashiro. Spatio-Temporal Scaling of Turbulent Photospheric Line-of-Sight Magnetic Field in Active Region NOAA 11158. *Solar Physics*, 290(2):335–350, 2015.

[15] R. J. Harris and G. M. Schütz. Fluctuation theorems for stochastic dynamics. *Journal of Statistical Mechanics: Theory and Experiment*, 2007(07):P07020–P07020, July 2007.

[16] P. S. Iroshnikov. Turbulence of a Conducting Fluid in a Strong Magnetic Field. *Soviet Astronomy*, 7:566, February 1964.

[17] K. Janßen, A. Vögler, and F. Kneer. On the fractal dimension of small-scale magnetic structures in the Sun. *Astronomy & Astrophysics*, 409(3):1127–1134, October 2003.

[18] Christopher Jarzynski. Equalities and Inequalities: Irreversibility and the Second Law of Thermodynamics at the Nanoscale. *Annual Review of Condensed Matter Physics*, 2(1):329–351, March 2011.

[19] Rainer Klages, W. Just, and Christopher Jarzynski, editors. *Nonequilibrium Statistical Physics of Small Systems: Fluctuation Relations and Beyond*. Reviews of Nonlinear Dynamics and Complexity. Wiley-VCH Verlag GmbH & Co. KGaA, Weinheim, Germany, 2013.

[20] A. N. Kolmogorov. A refinement of previous hypotheses concerning the local structure of turbulence in a viscous incompressible fluid at high Reynolds number. *Journal of Fluid Mechanics*, 13(1):82–85, 1962.

[21] A. N. Kolmogorov. Dokl. Akad. Nauk SSSR 31, 538 (1941) [Proc. R. Soc. London A 434, 15 (1991)].

[22] Robert H. Kraichnan. Inertial-Range Spectrum of Hydromagnetic Turbulence. *Physics of Fluids*, 8:1385–1387, July 1965.

[23] Y. Liu, J. T. Hoeksema, P. H. Scherrer, J. Schou, S. Couvidat, R. I. Bush, T. L. Duvall, K. Hayashi, X. Sun, and X. Zhao. Comparison of Line-of-Sight Magnetograms Taken by the Solar Dynamics Observatory/Helioseismic and Magnetic Imager and Solar and Heliospheric Observatory/Michelson Doppler Imager. *Solar Physics*, 279(1):295–316, July 2012.

[24] Umberto Marini Bettolo Marconi, Andrea Puglisi, Lamberto Rondoni, and Angelo Vulpiani. Fluctuation–dissipation: Response theory in statistical physics. *Physics Reports*, 461(4):111–195, June 2008.

[25] C. Meneveau and K. R. Sreenivasan. Simple multifractal cascade model for fully developed turbulence. *Physical Review Letters*, 59(13):1424–1427, 1987.

[26] H. Politano and A. Pouquet. Model of intermittency in magnetohydrodynamic turbulence. *Physical Review E*, 52(1):636–641, July 1995.

[27] François Rincon and Michel Rieutord. The Sun's supergranulation. *Living Reviews in Solar Physics*, 15(1):6, 2018.

[28] Alexander A. Schekochihin. MHD turbulence: A biased review. *Journal of Plasma Physics*, 88(5):155880501, October 2022.

[29] P. H. Scherrer, J. Schou, R. I. Bush, A. G. Kosovichev, R. S. Bogart, J. T. Hoeksema, Y. Liu, T. L. Duvall, J. Zhao, A. M. Title, C. J. Schrijver, T. D. Tarbell, and S. Tomczyk. The Helioseismic and Magnetic Imager (HMI) Investigation for the Solar Dynamics Observatory (SDO). *Solar Physics*, 275:207–227, January 2012.

[30] J. Schou, P. H. Scherrer, R. I. Bush, R. Wachter, S. Couvidat, M. C. Rabello-Soares, R. S. Bogart, J. T. Hoeksema, Y. Liu, T. L. Duvall, D. J. Akin, B. A. Allard, J. W. Miles, R. Rairden, R. A. Shine, T. D. Tarbell, A. M. Title, C. J. Wolfson, D. F. Elmore, A. A. Norton, and S. Tomczyk. Design and Ground Calibration of the Helioseismic and Magnetic Imager (HMI) Instrument on the Solar Dynamics Observatory (SDO). *Solar Physics*, 275(1-2):229–259, January 2012.

[31] Jörg Schumacher and Katepalli R. Sreenivasan. Colloquium: Unusual dynamics of convection in the Sun. *Reviews of Modern Physics*, 92:041001, October 2020.

[32] Udo Seifert. Stochastic thermodynamics, fluctuation theorems and molecular machines. *Reports on Progress in Physics*, 75(12):126001, December 2012.

[33] Udo Seifert. From stochastic thermodynamics to thermodynamic inference. *Annual Review of Condensed Matter Physics*, 10(1):171–192, March 2019.

[34] Zhen-Su She. Hierarchical structures and scalings in turbulence. In Oluş Boratav, Alp Eden, and Ayse Erzan, editors, *Turbulence Modeling and Vortex Dynamics*, Lecture Notes in Physics, pages 28–52, Berlin, Heidelberg, 1997. Springer.

[35] Zhen-Su She and Emmanuel Leveque. Universal scaling laws in fully developed turbulence. *Physical Review Letters*, 72(3):336–339, 1994.

[36] J. O. Stenflo. Scaling laws for magnetic fields on the quiet Sun. *Astronomy and Astrophysics*, 541:A17, 2012.

[37] G. Stolovitzky, P. Kailasnath, and K. R. Sreenivasan. Kolmogorov's refined similarity hypotheses. *Physical Review Letters*, 69(8):1178–1181, 1992.

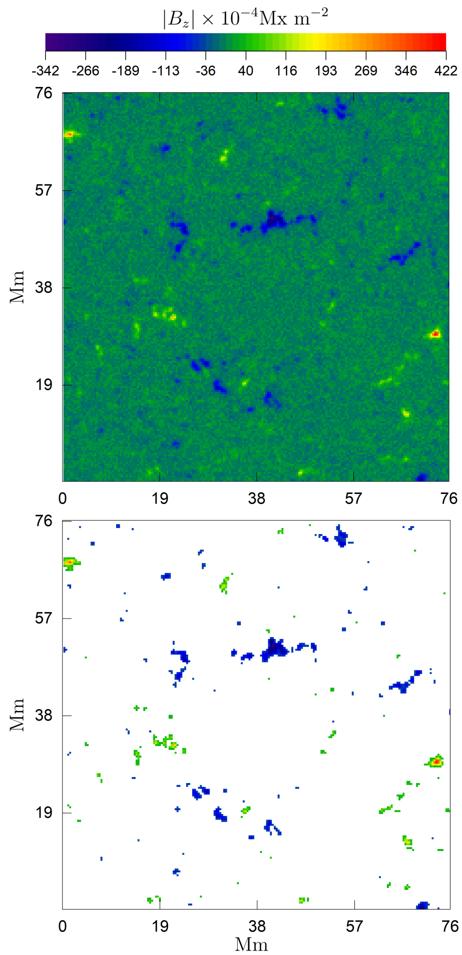

Figure 1: Top panel: the first magnetogram in the analyzed time-series with the FoV limited to 200^2 pixels. The spatial sampling on the solar surface is $\approx$ 380 km = 0.5 arcsec/pixel. The FoV is chosen to minimize B_z projection effects, spatial inhomogeneity of the noise, and other instrumental effects, as well as the solar differential rotation. Bottom panel: the same as above with the applied noise threshold cutoff of $3\sigma = 3 \times 10.3 \times 10^{-4}$ Mx m^{-2} [23]. The rounded structure of MFD concentrations in the center (approx. tens Mm scale) outlines supergranule boundaries, the so-called magnetic network [27]. The data analyzed here consist of $3,728,333$ stochastic trajectories from which 55% are trajectories with $\Delta s^{+}_{\mathrm{T}}$.

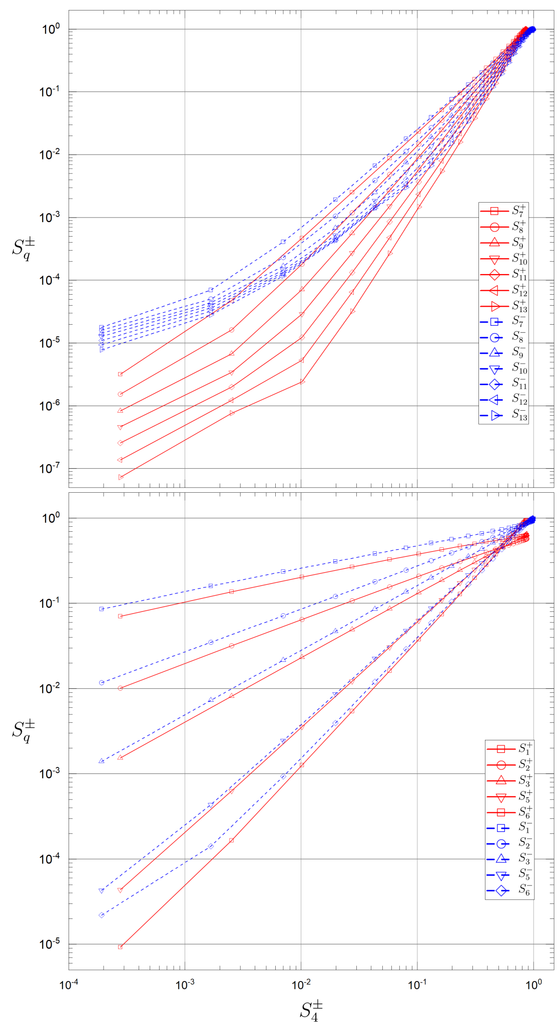

Figure 2: Normalized structure functions S_q of the order up to $q = 13$ are shown as functions of S_4. Dashed lines: structure functions for $\Delta s_{\mathrm{T}}^{+}$-trajectories. Solid lines: structure functions for $\Delta s_{\mathrm{T}}^{-}$-trajectories. For clarity, functions are bounded by the upper limit of the inertial range.

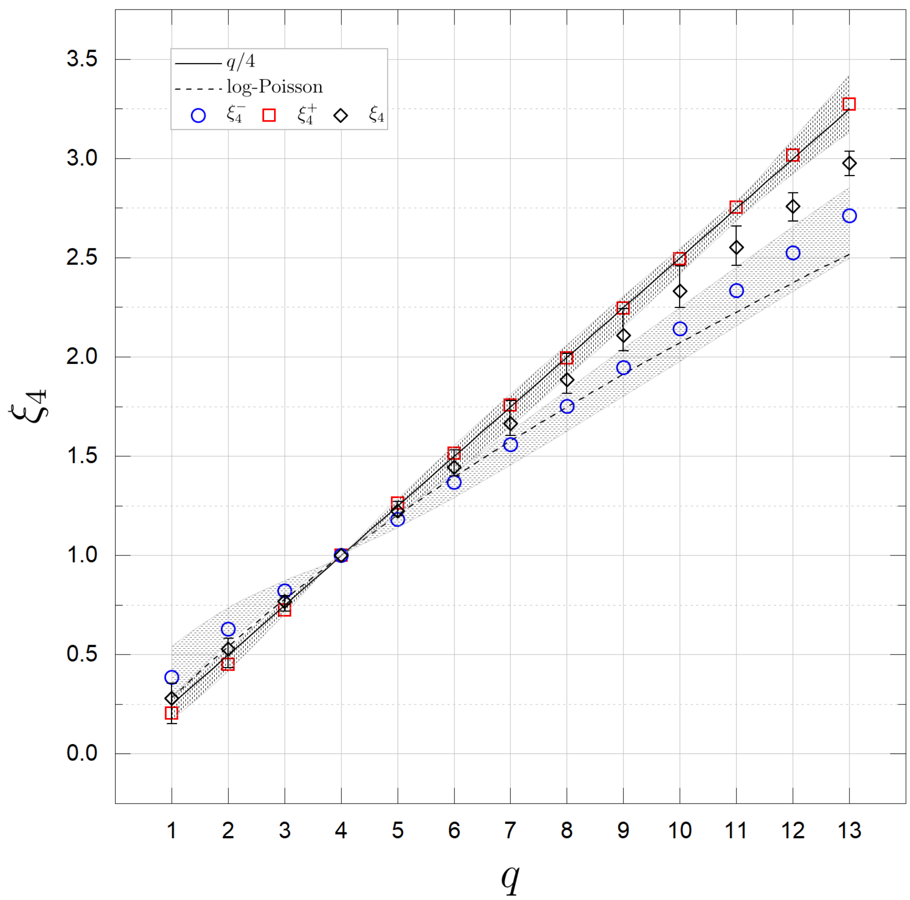

Figure 3: The relative scaling exponents ξ_4 as functions of SF order q for sets of $\Delta s_{\mathrm{T}}^{+}$-trajectories (squares), $\Delta s_{\mathrm{T}}^{-}$-trajectories (circles), and the joint data set (diamonds). Bars and shadowed regions are the $99,99\%$ confidence intervals computed for χ^2 merit functional. Lines are the model values with the MHD linear scaling (solid) and the anomalous scaling according to Eq. (10) (dashed).